Am J Cancer Res 2023;13(2):464-474
www.ajcr.us /ISSN:2156-6976/ajcr0147840

Original Article

SIRT6 drives sensitivity to ferroptosis in anaplastic thyroid cancer through NCOA4-dependent autophagy

Zhou Yang[1,2*], Renhong Huang[3*], Yunjun Wang[1,2], Qing Guan[1,2], Duanshu Li[1,2], Yi Wu[1,2], Tian Liao[1,2], Yu Wang[1,2], Jun Xiang[1,2]

[1]Department of Head and Neck Surgery, Fudan University Shanghai Cancer Center, Shanghai 200032, China; [2]Department of Oncology, Shanghai Medical College, Fudan University, Shanghai 200032, China; [3]Department of General Surgery, Comprehensive Breast Health Center, Ruijin Hospital, Shanghai Jiao Tong University School of Medicine, Shanghai 200025, China. [*]Equal contributors.

Received November 18, 2022; Accepted January 26, 2023; Epub February 15, 2023; Published February 28, 2023

Abstract: The sirtuin family has been reported to participate in the regulation of oxidative stress, cancer metabolism, aging, and so on. However, few studies have demonstrated its role in ferroptosis. Our previous studies confirmed that SIRT6 is upregulated in thyroid cancer and associated with cancer development by regulating glycolysis and autophagy. In this research, we aimed to elucidate the association between SIRT6 and ferroptosis. RSL3, erastin, ML210, and ML162 were applied to induce ferroptosis. Cell death and lipid peroxidation were measured by flow cytometry. We found that overexpression of SIRT6 significantly increased the sensitivity of cells to ferroptosis, whereas knockout of SIRT6 promoted resistance to ferroptosis. Furthermore, we demonstrated that SIRT6 induced NCOA4-dependent autophagic degradation of ferritin, thus driving sensitivity to ferroptosis. The clinically used ferroptosis inducer sulfasalazine showed promising therapeutic effects on SIRT6-upregulated thyroid cancer cells in vivo. In conclusion, our research demonstrated SIRT6-driven sensitivity to ferroptosis via NCOA4-dependent autophagy and proposed ferroptosis inducers as promising therapeutic agents for anaplastic thyroid cancer patients.

Keywords: Sirtuins, SIRT6, ferroptosis, autophagy, anaplastic thyroid cancer

Introduction

Thyroid cancer is a common malignant tumor with an increased incidence in recent years and has four pathological types: papillary carcinoma (PTC), follicular carcinoma (FTC), anaplastic/undifferentiated carcinoma (ATC), and medullary carcinoma (MTC) [1]. Among these types, ATC is one of the most malignant thyroid cancers, with a high invasion ability and poor prognosis. Moreover, ATC patients derive little benefit from surgery, drugs, radiotherapy, and chemotherapy. Therefore, new intervention strategies are needed for ATC patients [2].

Ferroptosis is an iron dependent, new type of programmed cell death that is different from apoptosis, necrosis, and autophagy and therefore has great therapeutic potential in cancer. Through the action of divalent iron or ester oxygenase, the oxidation of unsaturated fatty acids highly expressed on the cell membrane is catalyzed to induce lipid peroxidation, thereby inducing cell death [3, 4]. Ferroptosis is related to the occurrence and treatment response of various types of tumors. Experimental reagents (such as erastin and RSL3), approved drugs (such as sorafenib, sulfasalazine, statins, and artemisinin), ionizing radiation, and cytokines (such as IFNγ and TGFβ1) can induce ferroptosis and inhibit tumor growth [5, 6]. Cancer cells maintain a labile iron pool by coordinating iron uptake, utilization, storage, and export, which is critical for the regulation of ferroptosis. Intracellular iron is mainly stored in ferritin in the form of inert iron, and nuclear receptor coactivator 4 (NCOA4)-mediated autophagic degradation of ferritin releases the iron stored in ferritin into unstable iron pools, thereby promoting ferroptosis [7].

The sirtuin family contains nicotinamide adenine dinucleotide (NAD^+)-dependent histone deacetylases and consists of 7 members (SIRT1-

7), each of which has different localizations and functions. The sirtuin family has been reported to participate in the development of various cancers by regulating metabolism, aging, oxidative stress, and so on [8-10]. However, few studies have reported the association of Sirtuins and ferroptosis. Our previous studies demonstrated that SIRT6 is upregulated in thyroid cancer and participates in cancer development by regulating multiple mechanisms, including autophagy, glycolysis, and oxidative stress [11, 12]. In this research, we aimed to elucidate the association between SIRT6 and ferroptosis.

Material and methods

Cell culture and reagents

The human ATC cell lines CAL62 and BHT101 were purchased from the University of Colorado Cancer Center Cell Bank. The cells were cultured in DMEM supplemented with 10% FBS (Invitrogen, Carlsbad, CA, USA) at 37°C in a 5% CO_2 atmosphere.

Nicotinamide, RSL3, Erastin, ML210, ML162, ferrostatin-1, chloroquine (CQ), and sulfasalazine (SSZ) were purchased from MedChemExpress (Monmouth Junction, NJ, USA).

Measurement of cell viability, cell death and lipid peroxidation

A total of 10^4 cells suspended in 100 µl medium were seeded into 96-well plates overnight. Then, the cells were treated with the required concentration of RSL3 for 24 h. Finally, cell viability was measured by the addition of 10 µl CCK8 reagent (Dojindo Molecular Technologies, Kumamoto, Japan) per well. After incubation for 2 hours, the absorbance of the wells was measured at a wavelength of 450 nm (OD450) using a Tecan Infinite M200 microplate reader (Tecan Co., Männedorf, Switzerland).

Measurement of cell death and lipid peroxidation

For measurement of lipid peroxidation and cell death, 10^6 cells suspended in 2 ml of medium were seeded in 6-well plates overnight. Then, the cells were treated with the required concentration of RSL3 for 24 h and incubated with 2 µM C11 BODIPY 581/591 (Invitrogen, Carlsbad, CA, USA) for the detection of lipid peroxidation or with 1 µg/mL propidium iodide (PI) (Invitrogen) in PBS for the detection of cell death. After washing twice with PBS, the cells were collected and then subjected to fluorescence-activated cell sorting (FACS) analysis using an Accuri C6 flow cytometer (BD biosciences, San Jose, CA, USA).

CRISPR/Cas9-mediated genome editing

For CRISPR/Cas9-mediated genome editing, single-guide RNAs (sgRNAs, sgSIRT6#1: TACGTCCGAGACACAGTCGT; sgSIRT6#2: TCCATGGTCCAGACTCCGTG; sgNCOA4: GTAAGGAGCTTGATAACCAC) were designed using the http://crispr.mit.edu website and inserted into the CRISPR-V2 vector (Addgene, #52961) [13]. Lentivirus packaging and infection were performed as described previously [14]. After screening with puromycin (2 µg/ml) for 72 h, single cells were sorted into 96-well plates to obtain single clones. Finally, the clones were validated by Sanger sequencing and Western blot analysis to obtain genome-edited cells.

Cell transfection

The pcDNA3.1-SIRT1-7 plasmids were purchased from HedgehogBio, Inc. (Shanghai, China). For transfection, 10^6 cells were seeded in 6 cm dishes and cultured at 37°C. After 18 h, 2 µg plasmid and 10 µl Lipofectamine 3000 (Invitrogen, Inc.) was added to the culture medium. Subsequently, the cells were further cultured at 37°C for 36 h. Sirtuin overexpression was validated by RT-qPCR as described previously [14]. The primers are listed in Table S1.

Western blot analysis

Total cellular protein from each group was extracted using RIPA lysis buffer with 1% phenylmethanesulfonyl fluoride (PMSF). Then, equal amounts (20 µg) of protein, as determined by a BCA protein assay kit (Thermo Fisher Scientific, Waltham, MA, USA), were separated using 10% SDS-PAGE gels. The proteins were then transferred to PVDF membranes (0.45 mm, Solarbio, Beijing, China). The membranes were blocked with 5% nonfat milk for 1 h at room temperature and then incubated with primary antibodies at 4°C for 12 h. Rabbit polyclonal antibodies specific for the following proteins were used: Tubulin, ACSL4, SLC7A11, GPX4, NCOA4, FTH (1:1000, Abclonal, Inc., China); DHODH, FSP1, LC3, p62 (1:1000,

Proteintech Group. Inc.); SIRT6 (1:4000, Abcam, UK). Anti-mouse and anti-rabbit antibodies conjugated to horseradish peroxidase (HRP) (1:4000, Proteintech Group. Inc.) were used as secondary antibodies. The secondary antibodies were used at a 1:4000 dilution, and the membranes were incubated with these antibodies for approximately 1 h at room temperature. The bands were visualized with ECL reagents (Thermo Fisher Scientific) and imaged with an Omega Lum G imaging system (Aplegen, USA).

Animal model

Six-week-old male BALB/c-nu mice were provided by Beijing Vital River Laboratory Animal Technology Co. Ltd. All detailed experimental procedures were approved by the Institutional Animal Care and Utilization Committee of Fudan University Pudong Animal Experimental Center. All mice were randomly divided into 6 equal groups (CAL62-NC-Blank, CAL62-NC-sulfasalazine, CAL62-NC-sulfasalazine+CQ; CAL62-SIRT6-Blank, CAL62-SIRT6-sulfasalazine, CAL62-SIRT6-sulfasalazine+CQ). CAL62-NC or CAL62-SIRT6 cells (5×10^6) suspended in 100 μl PBS were injected subcutaneously into the axilla of each nude mouse. After 5 days, the mice were treated with different reagents: solvent (100 μl 0.1 M NaOH and 100 μl saline), sulfasalazine (200 mg/kg, i.p., dissolved in 100 μl 0.1 M NaOH), CQ (50 mg/kg, i.p., dissolved in 100 μl saline). The long (L) and short (S) diameters of the tumors were measured with Vernier calipers every 3 days (tumor volume = $L^*S^2/2$). The growth curve of the subcutaneous tumors was generated on the basis of the measured tumor volumes. All mice were euthanized by rapid cervical dislocation after 3 weeks. The xenografts were sliced into paraffin sections for immunohistochemical (IHC) staining. IHC staining was performed as described previously using anti-SIRT6, anti-NCOA4, and anti-4-HNE antibodies (1:100, Abcam, UK) [14]. An H-score was calculated using the following formula: H-score = $\sum$ (PI × I) = (percentage of cells of weak intensity × 1) + (percentage of cells of moderate intensity × 2) + percentage of cells of strong intensity × 3) [15].

Statistical analysis

All experiments were performed at least 3 times. SPSS software (version 19.0, IBM Corp., Armonk, NY, USA) was used for statistical analysis of all the experimental data. GraphPad Prism (version 7, GraphPad Software, La Jolla, CA, USA) was used to visualize the statistical results. All data are expressed as the mean + standard deviation (mean + sd) values. Statistical analysis of data from 2 groups was performed using a t test. Comparisons among multiple groups were performed by one-way ANOVA followed by the LSD-t test. $P<0.05$ was considered to be significant.

Results

Sirtuin family members regulate the response to ferroptosis

To further investigate the role of sirtuins in ferroptosis, we induced ferroptosis in thyroid cancer cell lines using RSL3 (0-2 μM, 24 h) combined with the pansirtuin inhibitor nicotinamide (5 mM, 24 h). Interestingly, cotreatment with nicotinamide alleviated the lethal effect of RSL3 (**Figure 1A**, **1B**). To further determine the role of each member of the sirtuin family (1-7), we separately overexpressed SIRT1-7 in CAL62 cells (**Figure 1C**). We found that overexpression of any Sirtuin (SIRT1-7) did not affect cell viability in the short term (24 h). Moreover, overexpression of SIRT3, 6, or 7 promoted the lethal and lipid peroxidation-inducing effects of RSL3, and the ferroptosis inhibitor ferrostatin-1 (Fer1) reversed the increase in the lethal effect (**Figure 1D-F**). Among the sirtuins, SIRT6 showed the strongest sensitizing effect on ferroptosis. Furthermore, we measured the expression of SIRT6 in CAL62 cells treated with RSL3 for different times. After the addition of RSL3, the expression of SIRT6 increased rapidly after the 2 h time point. Overexpression of SIRT6 lasted until the 24 h time point, with loss of total protein induced by the severe cell death (**Figure 1G**, **1H**).

SIRT6 promotes sensitivity to ferroptosis

To further investigate the role of SIRT6 in ferroptosis, we generated CAL62 and BHT101 cell lines with stable SIRT6 overexpression (**Figure 2A**). We found that overexpression of SIRT6 significantly augmented the lethal effect of RSL3 at different concentrations (0-2 μM) (**Figure 2B**). Additionally, we found that overexpression of SIRT6 promoted lipid peroxidation in both BHT101 and CAL62 cells. Treatment with RSL3

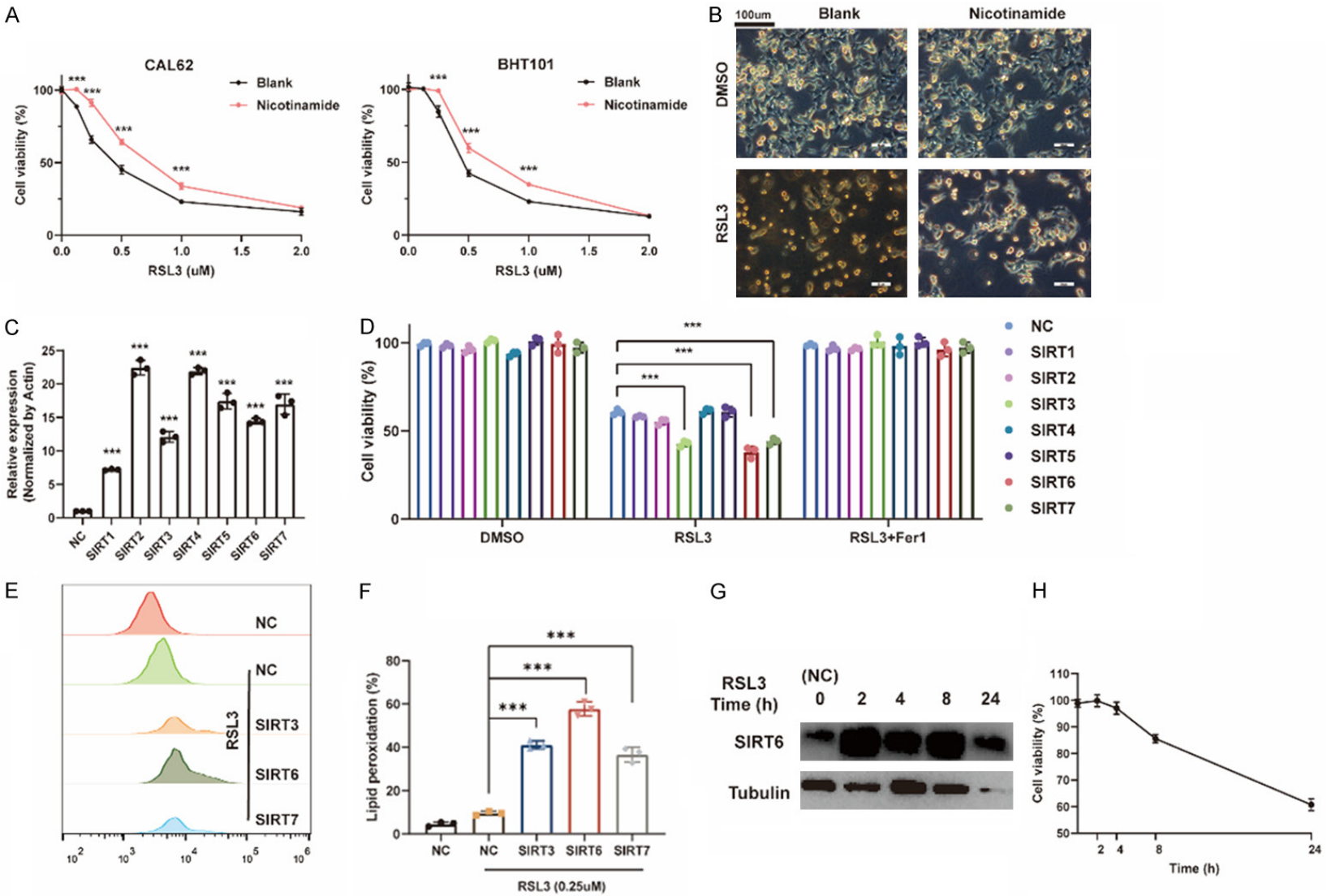

Figure 1. The sirtuin family regulates the response to ferroptosis. A. Viability of BHT101 and CAL62 cells treated with multiple concentrations of RSL3 (0-2 μM, 24 h) combined with the pansirtuin inhibitor nicotinamide (5 mM, 24 h). The viability of cells treated with different concentrations of RSL3 was normalized to the viability of cells without RSL3 treatment (0 μM). B. Representative images of CAL62 cells cotreated with RSL3 (0.5 μM, 24 h) and nicotinamide (5 mM, 24 h). C. Overexpression of SIRT1-7 in CAL62 cells was validated by RT-qPCR. CAL62 cells were transfected with pCDNA3.1 vectors (SIRT1-7, and NC: negative control). D. Viability of CAL62 cells (transfected with SIRT1-7) treated with RSL3 (0.5 μM, 24 h) and ferrostatin-1 (Fer1, 5 μM, 24 h). E. Lipid peroxidation in CAL62 cells (transfected with SIRT3/6/7) treated with RSL3 (0.5 μM, 24 h). F. Quantification of lipid peroxidation. G. The expression of SIRT6 in CAL62 cells treated with RSL3 (0.5 μM) for different times (0-24 h). H. Viability of CAL62 cells treated with RSL3 (0.5 μM) for different times (0-24 h) (***P<0.001).

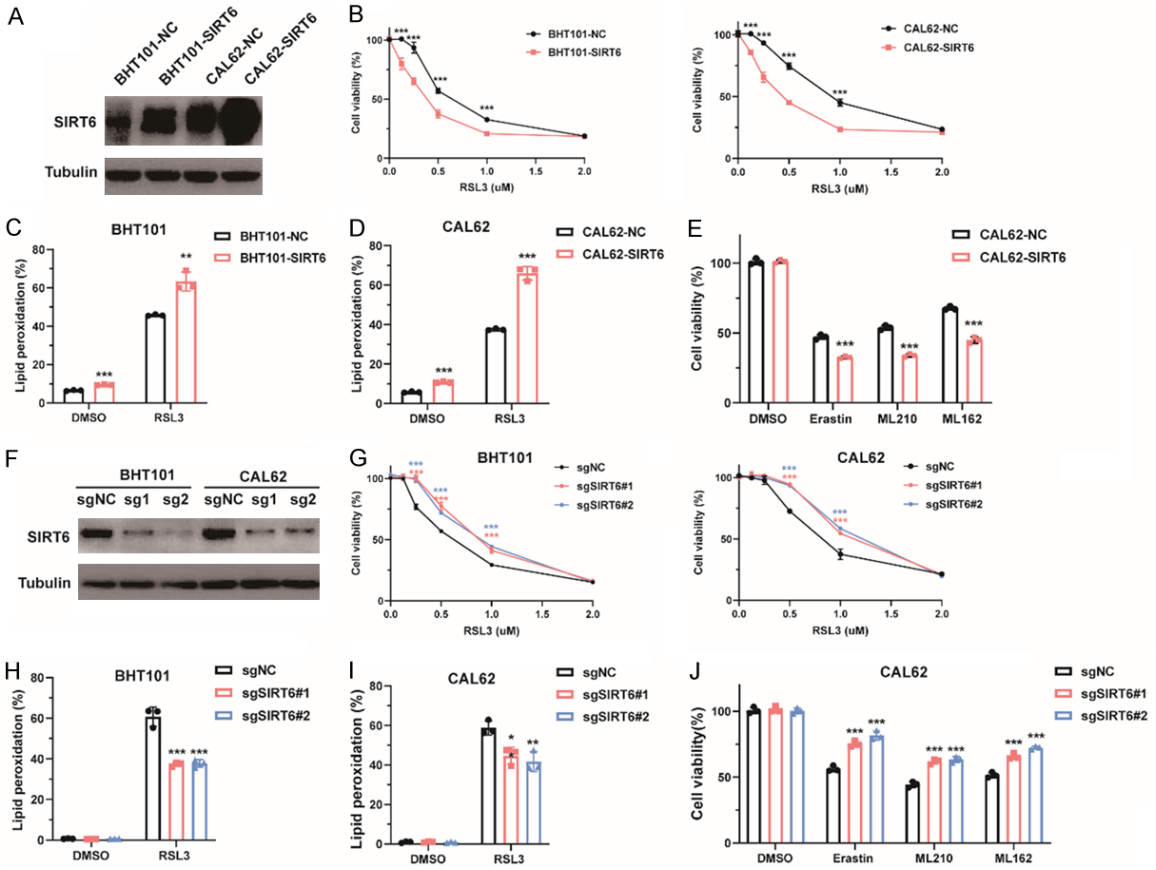

Figure 2. SIRT6 promotes sensitivity to ferroptosis. A. Overexpression of SIRT6 in BHT101 and CAL62 cells was validated by Western blotting. B. Viability of BHT101 and CAL62 cells treated with multiple concentrations of RSL3 (0-2 μM, 24 h). C. Lipid peroxidation in BHT101 cells treated with RSL3 (0.3 μM). DMSO was used as a control. D. Lipid peroxidation in CAL62 cells treated with RSL3 (0.3 μM). E. Viability of CAL62 cells treated with different FINs (Erastin, 20 μM; ML210, 2 μM; ML162, 2 μM; all treated for 24 h). F. Knockout of SIRT6 in BHT101 and CAL62 cells was validated by Western blotting. G. Viability of BHT101 and CAL62 cells treated with multiple concentrations of RSL3. H. Lipid peroxidation in BHT101 cells treated with RSL3 (0.3 μM). I. Lipid peroxidation in CAL62 cells treated with RSL3 (0.3 μM). J. Viability of CAL62 cells treated with different FINs (**P<0.01, ***P<0.001).

further augmented the promoting effect (**Figure 2C**, **2D**). Overexpression of SIRT6 also augmented the lethal effect of other ferroptosis inducers (FINs) in addition to RSL3, including erastin, ML210, and ML162 (**Figure 2E**). Furthermore, we knocked out the expression of SIRT6 to determine its role in ferroptosis (**Figure 2F**). As expected, SIRT6 knockout significantly suppressed the lethal effect of RSL3 and the lipid peroxidation induced by RSL3 in both BHT101 and CAL62 cells (**Figure 2G-I**). Knockout of SIRT6 also suppressed the lethal effect of other FINs in addition to RSL3 (**Figure 2J**).

SIRT6 sensitizes cells to ferroptosis by inducing autophagy

To demonstrate the mechanisms of the SIRT6-regulated ferroptosis response, we investigated the expression of the main ferroptosis regulators, including SLC7A11, ACSL4, GPX4, DHODH, and FSP1. Interestingly, SIRT6 showed no effect on the expression of these classical ferroptosis regulators. Previous research associated ferroptosis with NCOA4-mediated autophagy. NCOA4-mediated autophagic degradation of ferritin increases the cellular labile iron content, thus supporting ferroptosis [16]. Our previous results also confirmed that SIRT6 induced autophagy in papillary thyroid cancer cells via ROS [11]. Therefore, we hypothesized that SIRT6 regulates ferroptosis via NCOA4-mediated autophagy. As expected, overexpression of SIRT6 increased the ratio of LC3B II/I and promoted the expression of NCOA4 but suppressed the expression of p62 and ferritin heavy chain (FTH), indicating the activation of NCOA4-mediated autophagy (**Figure 3A**). We also demonstrated that the overexpression of

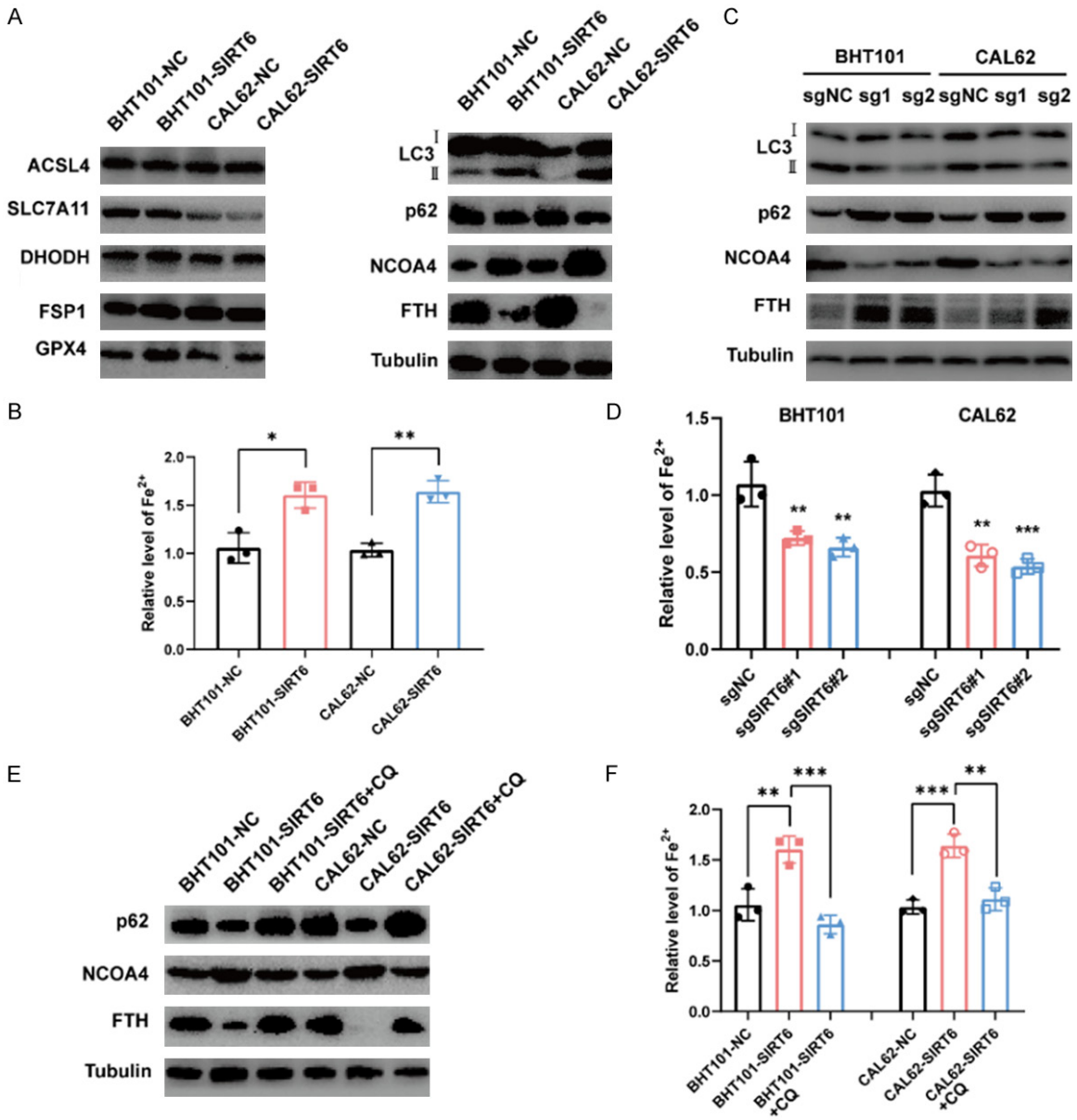

Figure 3. SIRT6 sensitizes cells to ferroptosis by inducing autophagy. A. The expression of classical ferroptosis regulators (ACSL4, SLC7A11, DHODH, FSP1, and GPX4) and NCOA4-mediated autophagy-associated proteins (LC3, p62, NCOA4, FTH) in SIRT6-overexpressing cell lines. B. Overexpression of SIRT6 increased the content of intracellular Fe^{2+}. C. The expression of NCOA4-mediated autophagy-associated proteins in SIRT6 knockout cell lines. D. Knockout of SIRT6 decreased the content of intracellular Fe^{2+}. E. Treatment with the autophagy inhibitor chloroquine (CQ, 5 μM for 24 h) rescued the expression of NCOA4-mediated autophagy-associated proteins. F. Treatment with the autophagy inhibitor CQ reversed the increase in intracellular Fe^{2+} in BHT101-SIRT6 and CAL-SIRT6 cells ($^{*}P<0.05$, $^{**}P<0.01$, $^{***}P<0.001$).

SIRT6 significantly increased the level of intracellular Fe^{2+}, suggesting the degradation of ferritin (**Figure 3B**). Furthermore, we also demonstrated that knockout of SIRT6 decreased the ratio of LC3B II/I and suppressed the expression of NCOA4 but promoted the expression of p62 and FTH (**Figure 3C**). Moreover, knockout of SIRT6 decreased the level of intracellular Fe^{2+} (**Figure 3D**). Subsequently, we treated SIRT6-overexpressing cell lines with the autophagy inhibitor chloroquine (CQ) to perform rescue experiments. As expected, treatment with CQ reversed the upregulation of NCOA4 and downregulation of FTH in BHT101-SIRT6 and CAL-SIRT6 cells (**Figure 3E**). Treatment with CQ also reversed the increase in intracellular Fe^{2+} in BHT101-SIRT6 and CAL-SIRT6 cells (**Figure 3F**).

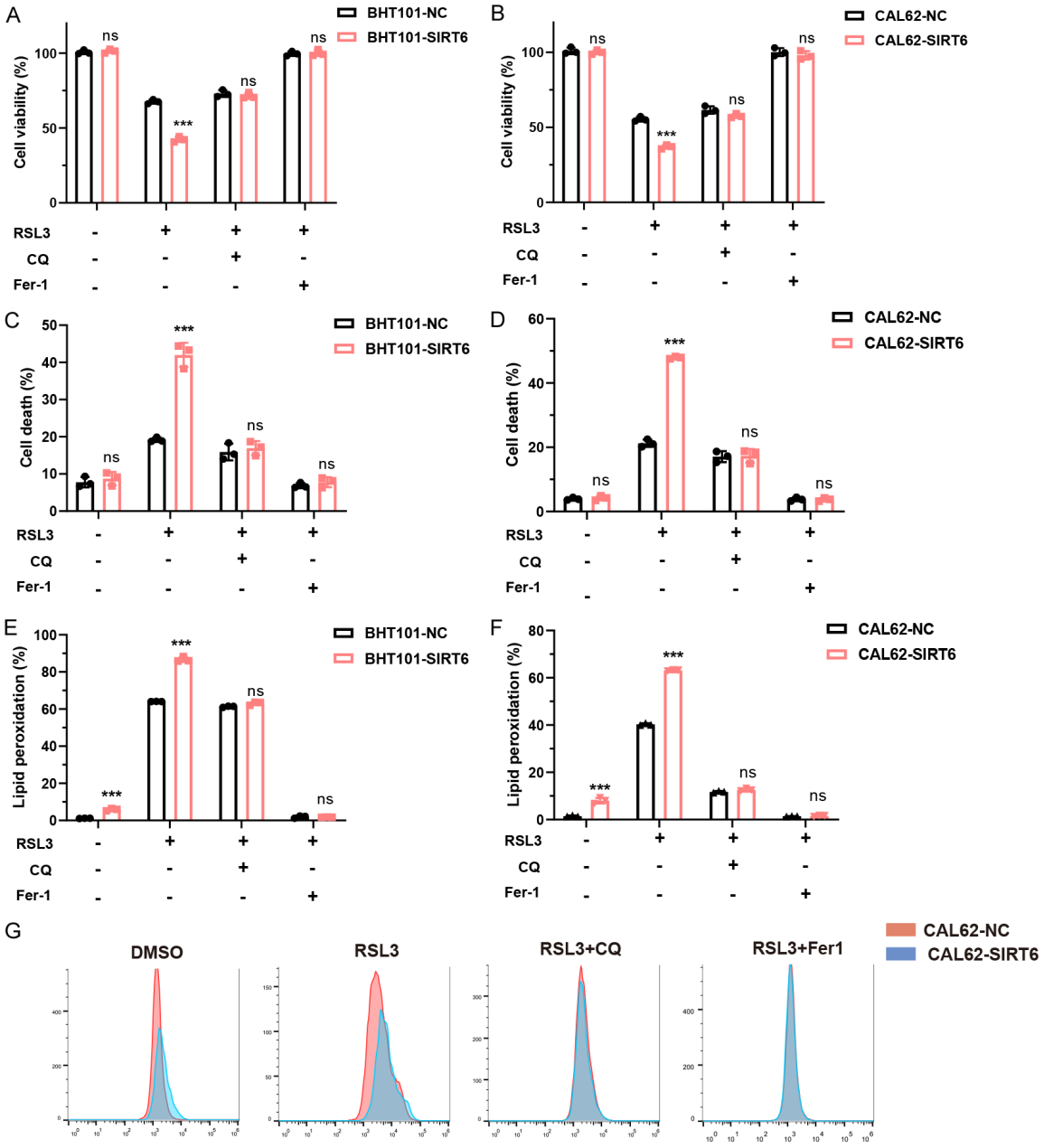

Figure 4. Autophagy contributes to SIRT6-regulated sensitization to ferroptosis. A, B. Viability of BHT101 and CAL62 cells treated with DMSO control (0.5 μM), RSL3 (0.5 μM), RLS3 (0.5 μM) and CQ (5 μM), RSL3 (0.5 μM) and Fer-1 (5 μM) for 24 h. C, D. Cell death in BHT101 and CAL62 cells treated with DMSO, RSL3, RLS3 and CQ, RSL3 and Fer-1 for 24 h. E-G. Lipid peroxidation in BHT101 and CAL62 treated with DMSO control, RSL3, RLS3 and CQ, RSL3 and Fer-1 for 24 h (*ns*: nonsignificant, ***P<0.001).

NCOA4-dependent autophagy contributes to SIRT6-regulated sensitization to ferroptosis

We further investigated cell viability, cell death, and lipid peroxidation in SIRT6 cell lines treated with autophagy inhibitor CQ or ferroptosis inhibitor Fer-1. Under the baseline condition (treatment with DMSO control), overexpression of SIRT6 showed no effect on cell viability and cell death but slightly promoted lipid peroxidation. With RSL3 treatment, overexpression of SIRT6 decreased cell viability but promoted cell death and lipid peroxidation. Interestingly, additional treatment of Fer-1 or CQ in RSL3-treated cells, the differences in cell viability, cell death, and lipid peroxidation were abolished (**Figure 4A-G**).

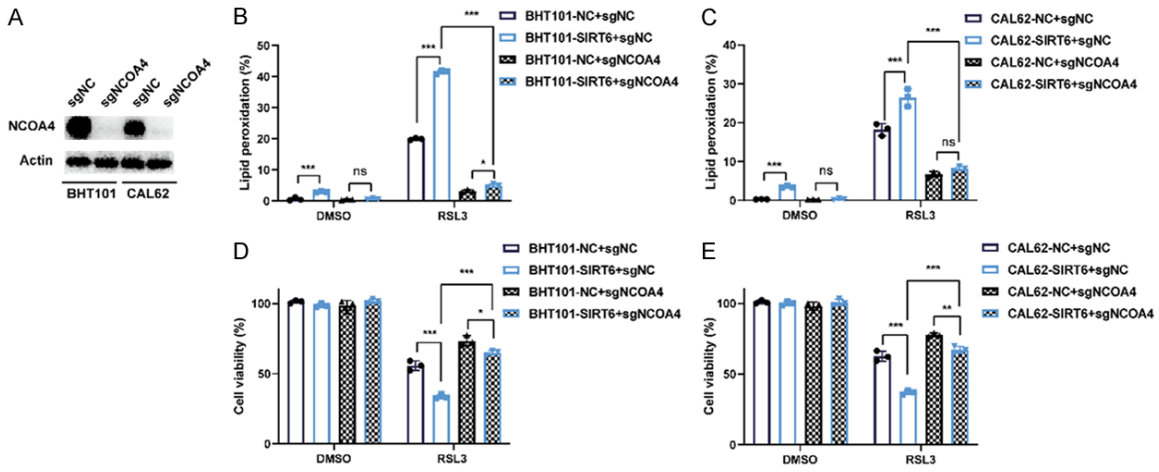

Figure 5. NCOA4-dependent autophagy contributes to SIRT6-regulated sensitization to ferroptosis. (A) Depletion of NCOA4 was validated by Western blotting. (B, C) Lipid peroxidation in NCOA4-depleted BHT101 cells (B) and CAL62 cells (C) treated with RSL3 (0.3 μM) for 24 h. (D, E) Viability of NCOA4-depleted BHT101 cells (D) and CAL62 cells (E) treated with RSL3 (0.5 μM) for 24 h (*ns*: nonsignificant, $^{*}P<0.05$, $^{**}P<0.01$, $^{***}P<0.001$).

These results indicated that SIRT6 sensitized cells to ferroptosis by inducing autophagy.

Moreover, we further investigated the role of NCOA4 in SIRT6-regulated ferroptosis sensitivity by genetic depletion (**Figure 5A**). Similar to addition of CQ, depletion of NCOA4 significantly suppressed the SIRT6mediated increase in ferroptosis sensitivity in both BHT101 and CAL62 cells (**Figure 5B-E**).

SIRT6 confers sensitivity to ferroptosis inducers in ATC in vivo

Finally, we further sought to determine the role of the SIRT6/ferroptosis axis and its therapeutic potential in ATC in vivo. Similar to the observation in our previous research, overexpression of SIRT6 slightly reduced the growth of ATC tumors in vivo (**Figure 6A-C**) [11]. Remarkably, by treating mice with sulfasalazine (SSZ), ferroptosis inducer used in vivo, the difference in growth was potently enhanced [17]. Mice implanted with SIRT6-overexpressing CAL62 xenograft tumors benefited more from SSZ, with enhanced ferroptosis in tumors (as indicated by increased staining of the lipid peroxidation marker 4-hydroxy-2-noneal [4-HNE], **Figure 6D**, **6F**). Moreover, additional treatment with CQ reversed the sensitizing effect of SIRT6 on SSZ (**Figure 6E**, **6F**).

Discussion

In our previous research, we demonstrated that SIRT6 was upregulated in papillary thyroid cancer and promoted cell invasion by regulating HIF-1α [18]. Additionally, SIRT6 was also found to regulate the Warburg effect in papillary thyroid cancer by inducing autophagy [11]. Of interest, we identified the association between SIRT6 and ferroptosis in this study. First, we found that treatment with a pansirtuin inhibitor promoted ferroptosis induced by RSL3. Further research confirmed that SIRT3, 6, and 7 contributed to this regulation. In gallbladder cancer cells and trophoblastic cells, SIRT3 has been confirmed to regulate ferroptosis via the Akt and AMPK pathways, respectively [19, 20]. Because SIRT6 showed the strongest sensitizing effect on ferroptosis, we further focused our research on its targetable vulnerability in ATC. As expected, overexpression of SIRT6 promoted but knockout of SIRT6 suppressed RSL3-induced ferroptosis in ATC cells.

Ferroptosis is regulated by several main processes or systems, including ACSL4-catalyzed peroxidation of polyunsaturated fatty acids (PUFAs), the GPX4-GSH system, the FSP1-CoQH2 system, the DHODH-CoQH2 system, and the cystine transporter SLC7A11/Xct [6, 21, 22]. Interestingly, SIRT6 showed no effect on any of these classical regulators/molecules. Our previous research demonstrated that SIRT6 induced autophagy by depleting histone H3 lysine 56 acetylation (H3K56ac) of negative regulator of reactive oxygen species (NRROS) [11]. Several studies have also confirmed that autophagy promotes ferroptosis via NCOA4-dependent autophagic degradation of ferritin.

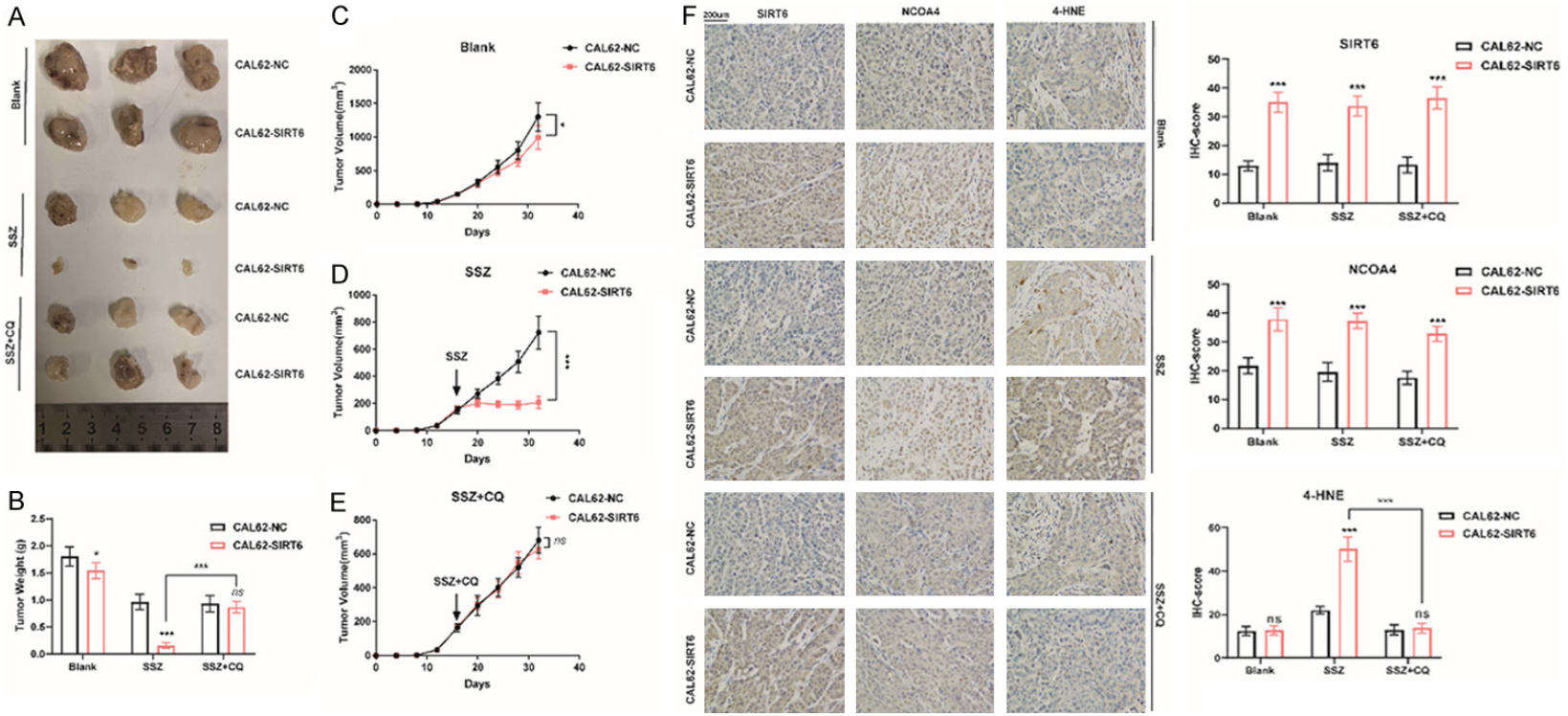

Figure 6. SIRT6 confers sensitivity to ferroptosis inducers in ATC in vivo. (A) Representative images of xenografts from each group (n = 6 mice per group). Blank group (100 μl 0.1 M NaOH and 100 μl saline per day), SSZ group (SSZ, 200 mg/kg per day), and SSZ+CQ group (200 mg/kg SSZ and 50 mg/kg CQ per day). (B) Weight of xenograft tumors in each group. (C-E) Growth curve of xenografts in each group: Blank group (C), SSZ group (D), and SSZ+CQ group (E). (F) IHC staining for SIRT6, NCOA4, and 4-HNE (a marker of lipid peroxidation) in xenografts in each group (*ns*: nonsignificant, $^{*}P<0.05$, $^{***}P<0.001$).

Iron is incorporated into ferritin in the form of Fe^{2+} through ferritin iron pores and is further oxidized to Fe^{3+} by ferritin heavy chain (FTH) [7]. Compared to Fe^{3+}, Fe^{2+} has stronger oxidizing properties and can participate in the Fenton reaction with ROS, thus resulting in lipid peroxidation and ferroptosis [23]. NCOA4 is an autophagy cargo receptor for ferritin; thus, it binds to ferritin and promotes its autophagic degradation. Depletion of NCOA4 inhibits ferritin delivery to lysosomes, thereby inhibiting ferritin degradation. Therefore, we hypothesized that SIRT6 regulates ferroptosis via autophagy in ATC cells. As expected, overexpression of SIRT6 induced NCOA4-dependent autophagic degradation of ferritin, thus increasing the level of Fe^{2+} and sensitizing cells to ferroptosis. The autophagy inhibitor CQ also successfully reversed SIRT6-mediated sensitization to ferroptosis. Finally, we confirmed that overexpression of SIRT6 promoted the response to SSZ, a ferroptosis inducer that inhibits SLC7A11. SSZ has been approved by the FDA and extensively tested in the treatment of inflammatory bowel disease and ankylosing spondylitis.

Conclusion

In conclusion, our research demonstrated that SIRT6 drives sensitivity to ferroptosis by inducing NCOA4-dependent autophagic degradation of ferritin in ATC. Considering the upregulation of SIRT6 in thyroid cancer patients, a ferroptosis inducer (sulfasalazine) may be a promising treatment agent.

Acknowledgements

The present study was funded by the Science and Technology Commission of Shanghai Municipality (20Y11914300), National Natural Science Foundation of China (82072951), Shanghai Hospital Development Center Clinical Research (SHDC2020CR6003), the Science and Technology Commission of Shanghai Municipality (22Y21900100 to Yu Wang) and the Shanghai Anticancer Association (SACA-AX202213 to Yu Wang).

Disclosure of conflict of interest

None.

Abbreviations

PTC, Papillary carcinoma; FTC, Follicular carcinoma; ATC, Anaplastic carcinoma; MTC, Medullary carcinoma; NCOA4, Nuclear receptor coactivator 4; NAD^+, Nicotinamide adenine dinucleotide; SIRT6, Sirtuin 6; SSZ, Sulfasalazine; FINs, Ferroptosis inducers; Fer1, Ferrostatin-1; CQ, Chloroquine; FTH, Ferritin heavy chain.

Address correspondence to: Jun Xiang, Yu Wang and Tian Liao, Department of Head and Neck Surgery, Fudan University Shanghai Cancer Center, No. 270, Dong'an Road, Shanghai 200032, China. E-mail: xiangjun@shca.org.cn (JX); neck130@hotmail.com (YW); liaotian@fudan.edu.cn (TL)

References

[1] Cabanillas ME, McFadden DG and Durante C. Thyroid cancer. Lancet 2016; 388: 2783-2795.

[2] Matsuzu K, Sugino K, Masudo K, Nagahama M, Kitagawa W, Shibuya H, Ohkuwa K, Uruno T, Suzuki A, Magoshi S, Akaishi J, Masaki C, Kawano M, Suganuma N, Rino Y, Masuda M, Kameyama K, Takami H and Ito K. Thyroid lobectomy for papillary thyroid cancer: long-term follow-up study of 1,088 cases. World J Surg 2014; 38: 68-79.

[3] Wu Z, Wu B, Lv X, Xie Y, Xu S, Ma C, Xu J, Tu X, Wei F and Chen H. Serumal lipidomics reveals the anti-inflammatory effect of flax lignans and sinapic acid in high-fat-diet-fed mice. J Agric Food Chem 2021; 69: 9111-9123.

[4] Bai Y, Meng L, Han L, Jia Y, Zhao Y, Gao H, Kang R, Wang X, Tang D and Dai E. Lipid storage and lipophagy regulates ferroptosis. Biochem Biophys Res Commun 2019; 508: 997-1003.

[5] Lei G, Zhuang L and Gan B. Targeting ferroptosis as a vulnerability in cancer. Nat Rev Cancer 2022; 22: 381-396.

[6] Chen X, Comish PB, Tang D and Kang R. Characteristics and biomarkers of ferroptosis. Front Cell Dev Biol 2021; 9: 637162.

[7] Mancias JD, Wang X, Gygi SP, Harper JW and Kimmelman AC. Quantitative proteomics identifies NCOA4 as the cargo receptor mediating ferritinophagy. Nature 2014; 509: 105-109.

[8] Shen J, Fang J, Hao J, Zhong X, Wang D, Ren H and Hu Z. SIRT1 inhibits the catabolic effect of IL-1beta through TLR2/SIRT1/NF-kappaB pathway in human degenerative nucleus pulposus cells. Pain Physician 2016; 19: E215-226.

[9] Kida Y and Goligorsky MS. Sirtuins, cell senescence, and vascular aging. Can J Cardiol 2016; 32: 634-641.

[10] Byles V, Zhu L, Lovaas JD, Chmilewski LK, Wang J, Faller DV and Dai Y. SIRT1 induces EMT by cooperating with EMT transcription factors and enhances prostate cancer cell mi-

gration and metastasis. Oncogene 2012; 31: 4619-4629.
[11] Yang Z, Huang R, Wei X, Yu W, Min Z and Ye M. The SIRT6-autophagy-Warburg effect axis in papillary thyroid cancer. Front Oncol 2020; 10: 1265.
[12] Qu N, Hu JQ, Liu L, Zhang TT, Sun GH, Shi RL and Ji QH. SIRT6 is upregulated and associated with cancer aggressiveness in papillary thyroid cancer via BRAF/ERK/Mcl1 pathway. Int J Oncol 2017; 50: 1683-1692.
[13] Hsu PD, Scott DA, Weinstein JA, Ran FA, Konermann S, Agarwala V, Li Y, Fine EJ, Wu X, Shalem O, Cradick TJ, Marraffini LA, Bao G and Zhang F. DNA targeting specificity of RNA-guided Cas9 nucleases. Nat Biotechnol 2013; 31: 827-832.
[14] Yang Z, Wang T, Wu D, Min Z, Tan J and Yu B. RNA N6-methyladenosine reader IGF2BP3 regulates cell cycle and angiogenesis in colon cancer. J Exp Clin Cancer Res 2020; 39: 203.
[15] Azim HA Jr, Peccatori FA, Brohee S, Branstetter D, Loi S, Viale G, Piccart M, Dougall WC, Pruneri G and Sotiriou C. RANK-ligand (RANKL) expression in young breast cancer patients and during pregnancy. Breast Cancer Res 2015; 17: 24.
[16] Yang M, Chen P, Liu J, Zhu S, Kroemer G, Klionsky DJ, Lotze MT, Zeh HJ, Kang R and Tang D. Clockophagy is a novel selective autophagy process favoring ferroptosis. Sci Adv 2019; 5: eaaw2238.
[17] Mao C, Liu X, Zhang Y, Lei G, Yan Y, Lee H, Koppula P, Wu S, Zhuang L, Fang B, Poyurovsky MV, Olszewski K and Gan B. DHODH-mediated ferroptosis defence is a targetable vulnerability in cancer. Nature 2021; 593: 586-590.
[18] Yang Z, Yu W, Huang R, Ye M and Min Z. SIRT6/HIF-1alpha axis promotes papillary thyroid cancer progression by inducing epithelial-mesenchymal transition. Cancer Cell Int 2019; 19: 17.
[19] Liu L, Li Y, Cao D, Qiu S, Li Y, Jiang C, Bian R, Yang Y, Li L, Li X, Wang Z, Ju Z, Zhang Y and Liu Y. SIRT3 inhibits gallbladder cancer by induction of AKT-dependent ferroptosis and blockade of epithelial-mesenchymal transition. Cancer Lett 2021; 510: 93-104.
[20] Han D, Jiang L, Gu X, Huang S, Pang J, Wu Y, Yin J and Wang J. SIRT3 deficiency is resistant to autophagy-dependent ferroptosis by inhibiting the AMPK/mTOR pathway and promoting GPX4 levels. J Cell Physiol 2020; 235: 8839-8851.
[21] Li Y, Feng D, Wang Z, Zhao Y, Sun R, Tian D, Liu D, Zhang F, Ning S, Yao J and Tian X. Ischemia-induced ACSL4 activation contributes to ferroptosis-mediated tissue injury in intestinal ischemia/reperfusion. Cell Death Differ 2019; 26: 2284-2299.
[22] Zhang Y, Swanda RV, Nie L, Liu X, Wang C, Lee H, Lei G, Mao C, Koppula P, Cheng W, Zhang J, Xiao Z, Zhuang L, Fang B, Chen J, Qian SB and Gan B. mTORC1 couples cyst(e)ine availability with GPX4 protein synthesis and ferroptosis regulation. Nat Commun 2021; 12: 1589.
[23] Gao M, Monian P, Pan Q, Zhang W, Xiang J and Jiang X. Ferroptosis is an autophagic cell death process. Cell Res 2016; 26: 1021-1032.

Table S1. The primers used for RT-qPCR

Gene	Forward Primer	Reverse Primer
SIRT1	TAGCCTTGTCAGATAAGGAAGGA	ACAGCTTCACAGTCAACTTTGT
SIRT2	TGCGGAACTTATTCTCCCAGA	GAGAGCGAAAGTCGGGGAT
SIRT3	ACCCAGTGGCATTCCAGAC	GGCTTGGGGTTGTGAAAGAAG
SIRT4	GCTTTGCGTTGACTTTCAGGT	CCAATGGAGGCTTTCGAGCA
SIRT5	GCCATAGCCGAGTGTGAGAC	CAACTCCACAAGAGGTACATCG
SIRT6	CCCACGGAGTCTGGACCAT	CTCTGCCAGTTTGTCCCTG
SIRT7	GACCTGGTAACGGAGCTGC	CGACCAAGTATTTGGCGTTCC
Actin	GGGACCTGACTGACTACCTC	TCATACTCCTGCTTGCTGAT